Supporting Information

UV-Vis-IR irradiation driven CO_2 reduction with high light-to-fuel efficiency on a unique nanocomposite of Ni nanoparticles loaded on Ni doped Al_2O_3 nanosheets

Qian Zhang, Yuanzhi Li, Shaowen Wu, Jichun Wu, Zhongkai Jiang, Yi Yang, Lu Ren, Xiujian Zhao*

State Key Laboratory of Silicate Materials for Architectures (Wuhan University of Technology), 122 Luoshi Road, Wuhan 430070, P. R. China. E-mail: liyuanzhi66@hotmail.com

Experimental

The η value was also calculated according to the standard molar Gibbs formation energy: [52]

$$\eta = (r_{H2} \times \Delta_f G^0_{H2} + r_{CO} \times \Delta_f G^0_{CO} - r_{CH4} \times \Delta_f G^0_{CH4} - r_{CO2} \times \Delta_f G^0_{CO2})/P$$

The values of $\Delta_f G^0_{H2}$, $\Delta_f G^0_{CO}$, $\Delta_f G^0_{CH4}$, and $\Delta_f G^0_{CO2}$ are 0, -137.2, -50.5, and -394.4 kJ mol^{-1}, respectively. The η value of Ni/Ni-Al_2O_3 with the focused UV-Vis-IR irradiation is 13.5%.

The η value according to $\Delta_f G^0$ being less than the corresponding values according to $\Delta_c H^0$ are ascribed to the following reason. As CRM is a reaction of entropy enhancement (ΔS_{298} =256.6 J K^{-1} mol^{-1}), its ΔG_{298} (170.5 kJ mol^{-1}) is less than its ΔH_{298} (247 kJ mol^{-1}) according to the Gibbs free energy equation ($\Delta G = \Delta H - T \times \Delta S$).

For perform photocatalytic CRM on Ni/Ni-Al_2O_3 at near ambient temperature under the focused UV-Vis-IR irradiation, the reactor was put in an ice-water bath.

The thermodynamic maximum η_{max} value of our reaction system is decided by Carnot efficiency as well as the solar absorption efficiency: [52, 55]

$$\eta_{max} = [1-\sigma \times T_H^4/(I_{DNI} \times C)] \times [1-T_L/T_H]$$

Where σ is Stefan–Boltzmann constant, I_{DNI} is the direct normal solar irradiation (1 kWm^{-2}), C is the concentration ratio of solar flux, T_H and T_L are the high and low temperatures of the equal Carnot heat engine.

In the present case, the focused UV-Vis-IR irradiation intensity was 333.8 kWm^{-2} (C is equal to 333.8). The focused UV-Vis-IR irradiation resulted in the surface temperature of Ni/Ni-Al_2O_3 being rapidly raised to an equilibrium temperature (T_H = 764 °C) from room temperature (T_L = 25 °C). The η_{max} value is calculated to be 57.2%.

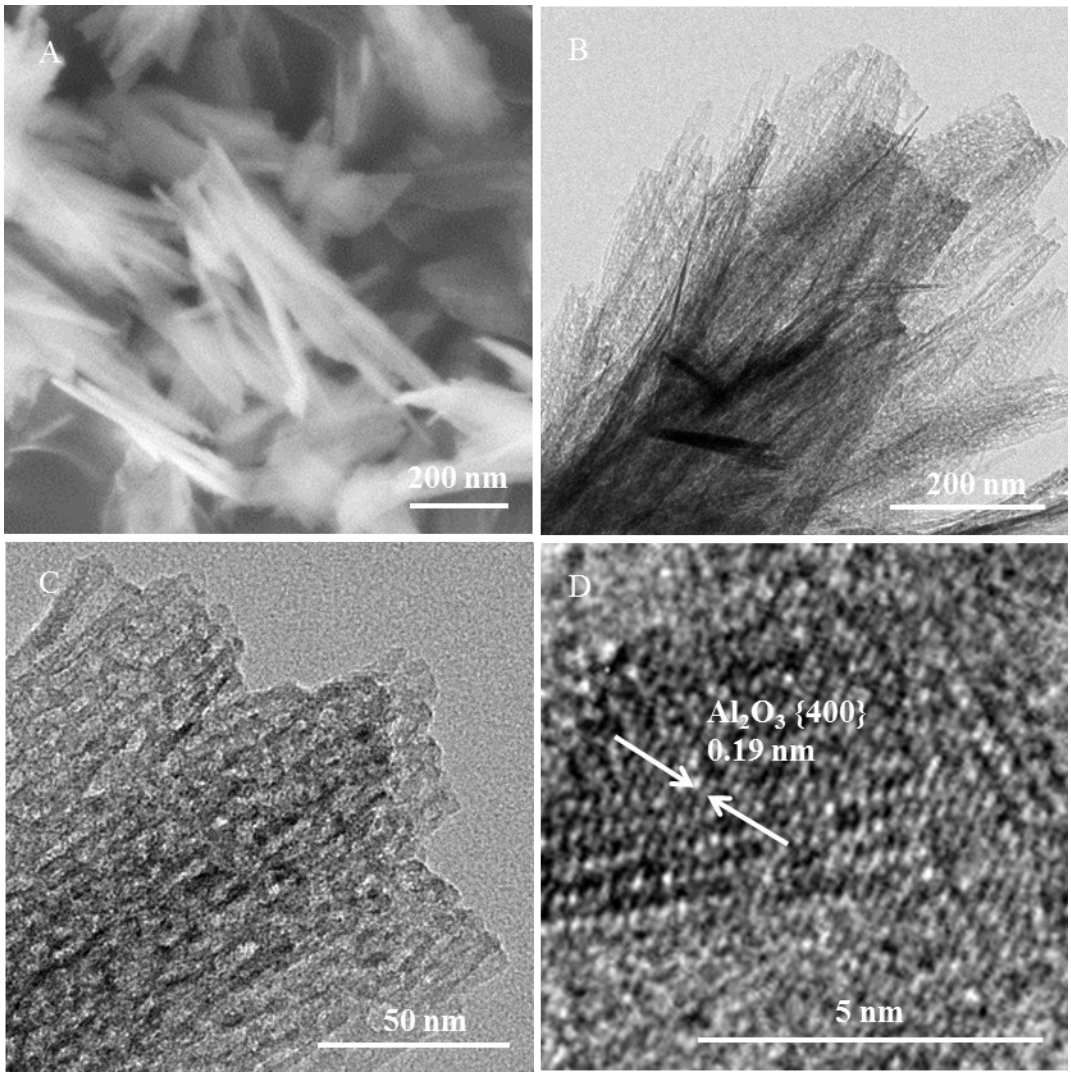

Figure S1. SEM image (A), TEM images (B, C), and HRTEM image (D) of Ni-Al_2O_3.

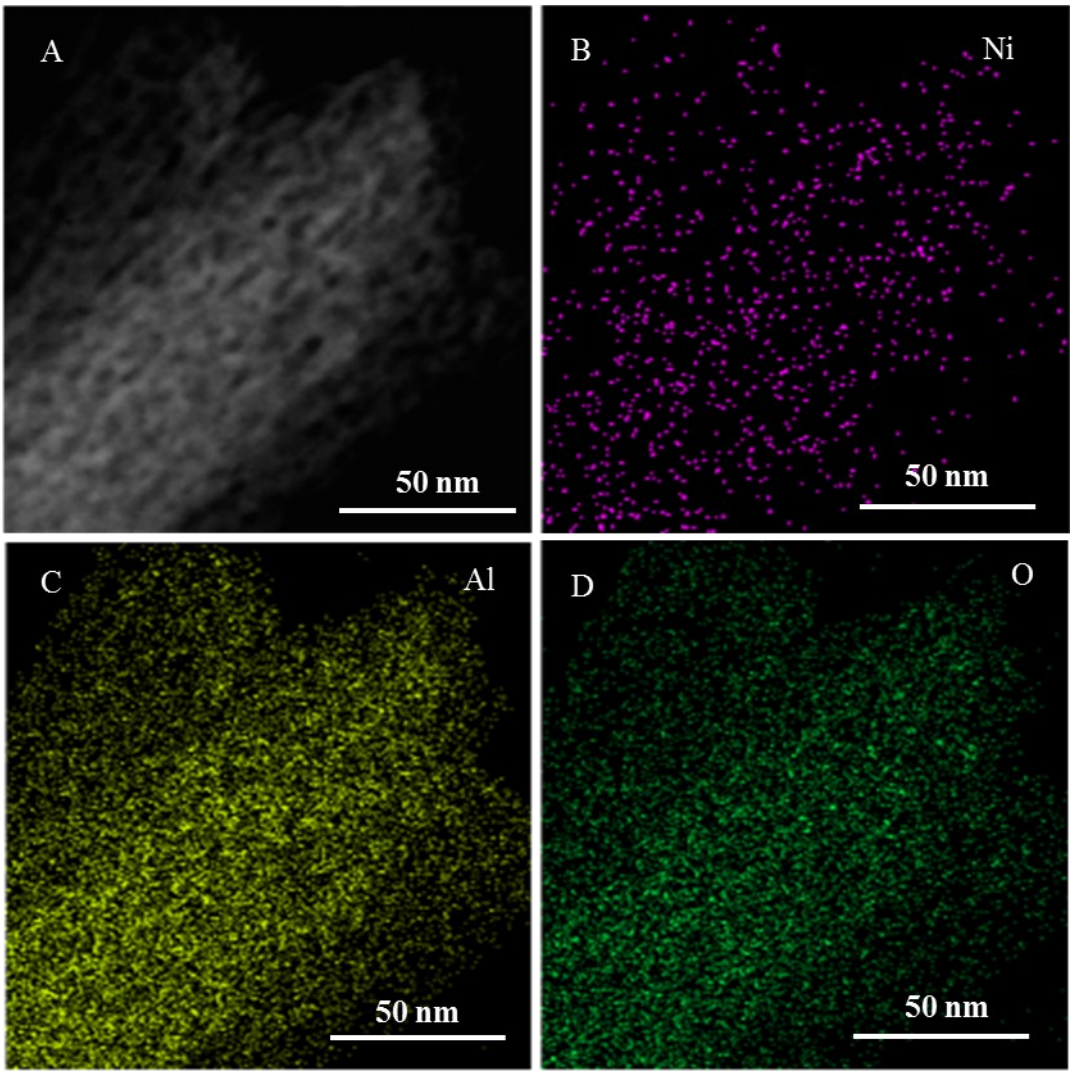

Figure S2. HAADF image (A) and the corresponding element mappings of Ni (B), Al (C), and O (D) of Ni-Al_2O_3.

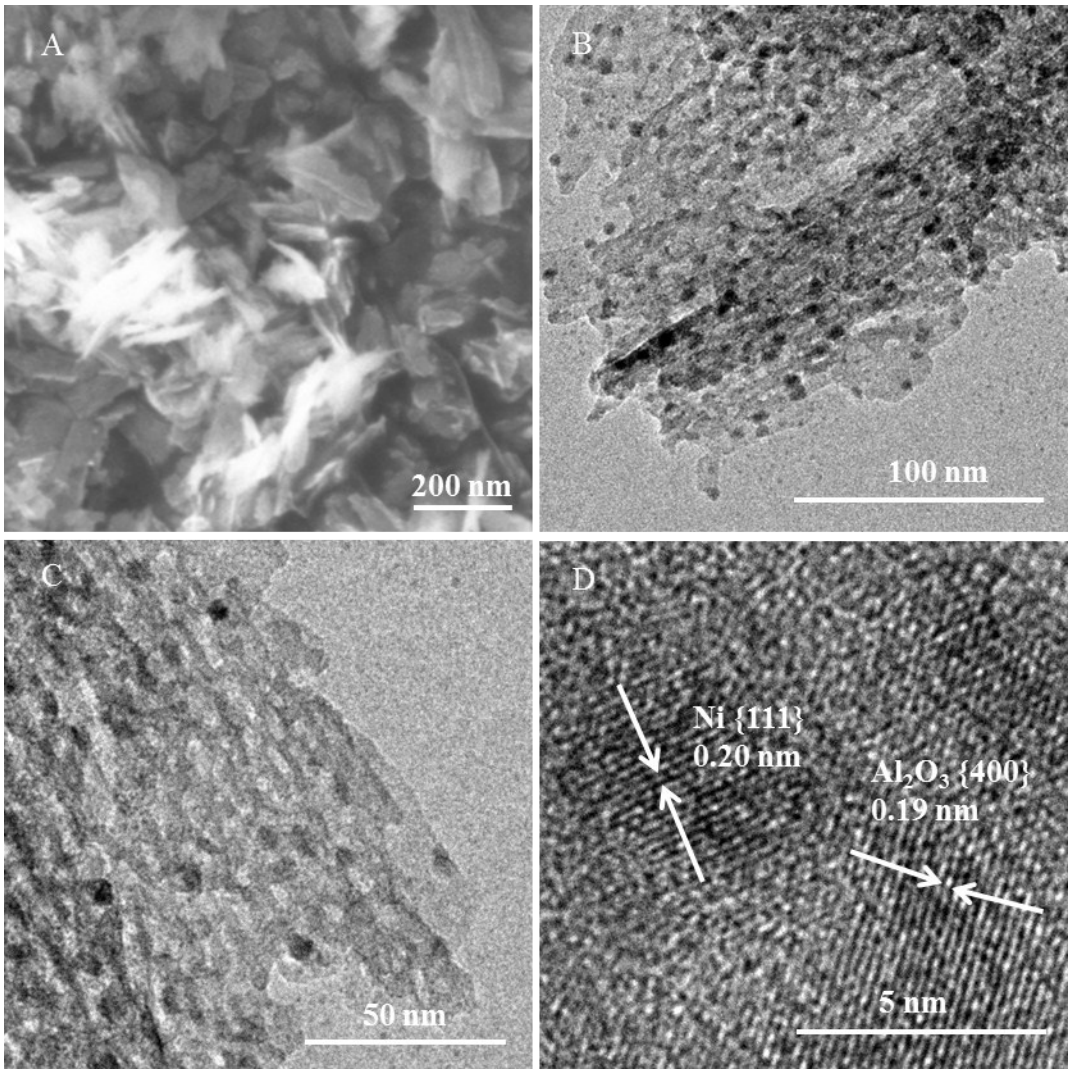

Figure S3. SEM image (A), TEM images (B, C), and HRTEM image (D) of Ni/Al_2O_3.

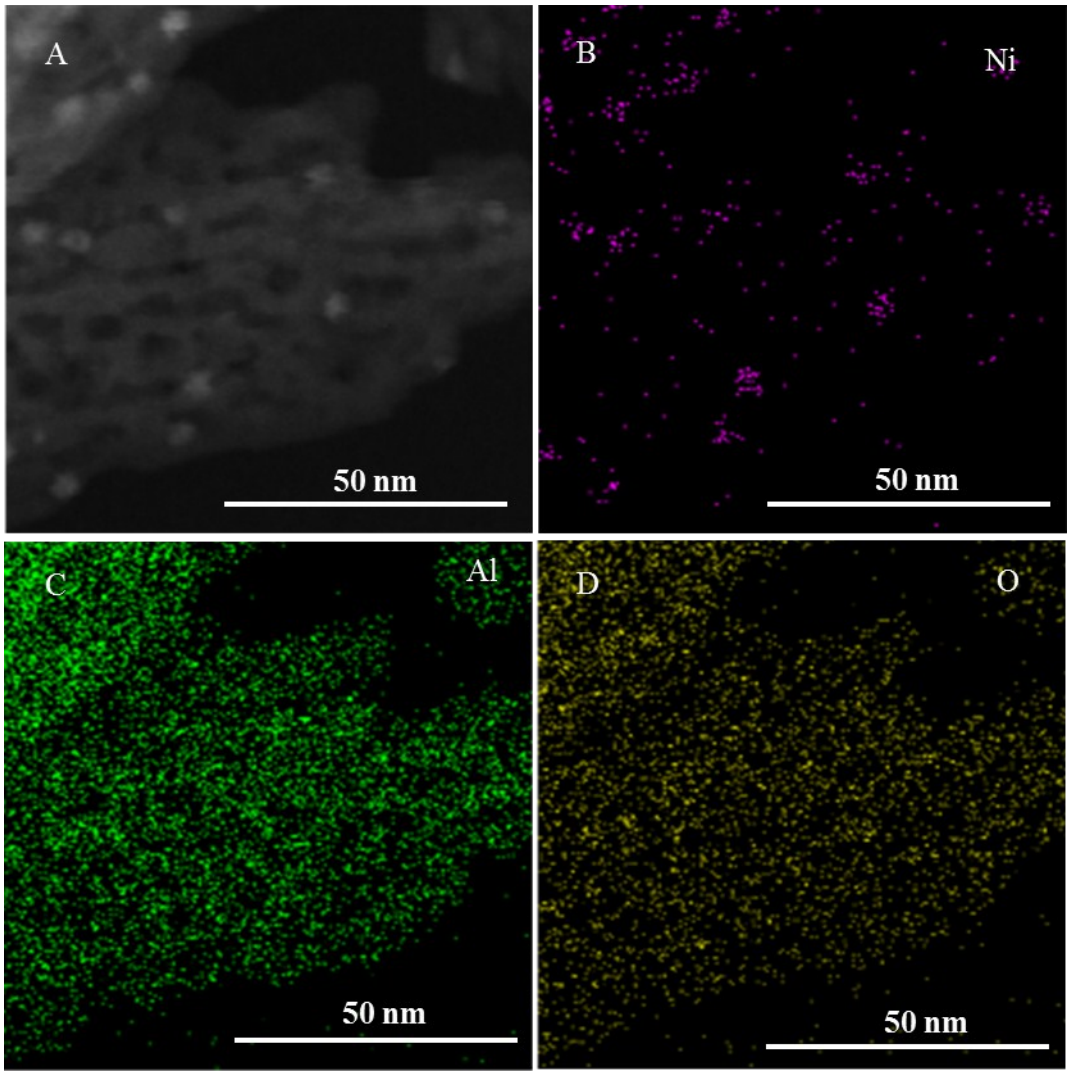

Figure S4. HAADF image (A) and the corresponding element mappings of Ni (B), Al (C), and O (D) of Ni/Al_2O_3.

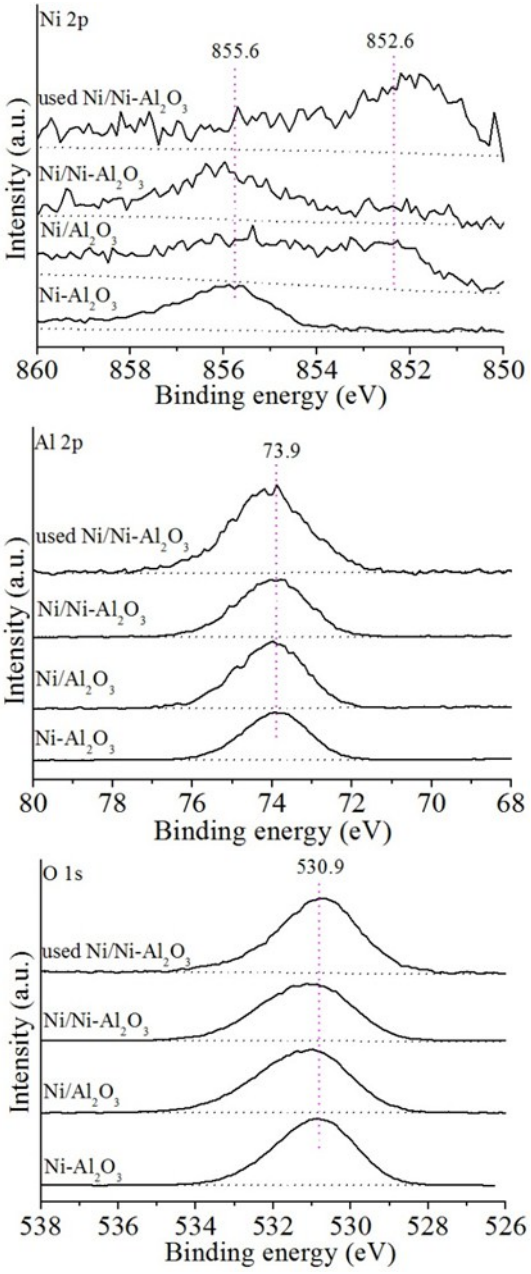

Figure S5. XPS spectra of Ni2p, Al2p, and O1s in Ni-Al_2O_3, Ni/Al_2O_3, Ni/$NiAl_2O_3$, and the used Ni/$NiAl_2O_3$ catalyst after the 80 h photothermocatalytic durability test.

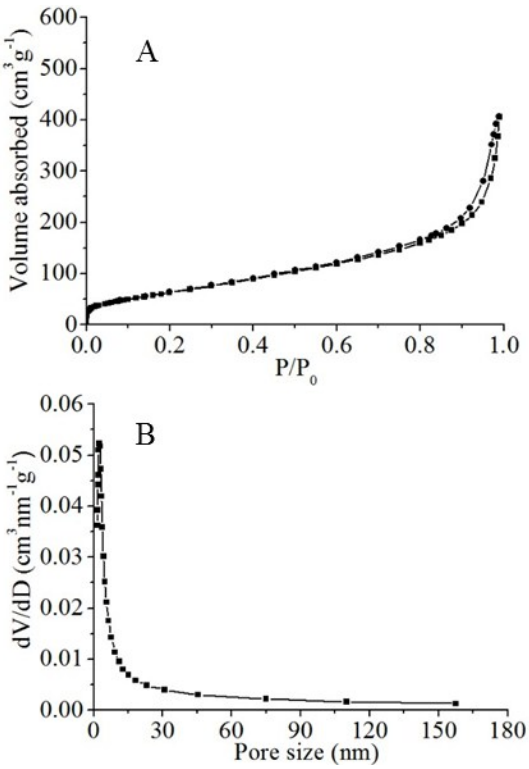

Figure S6. N_2 adsorption and desorption (A) and BJH adsorption pore size distribution (B) of Ni-Al_2O_3.

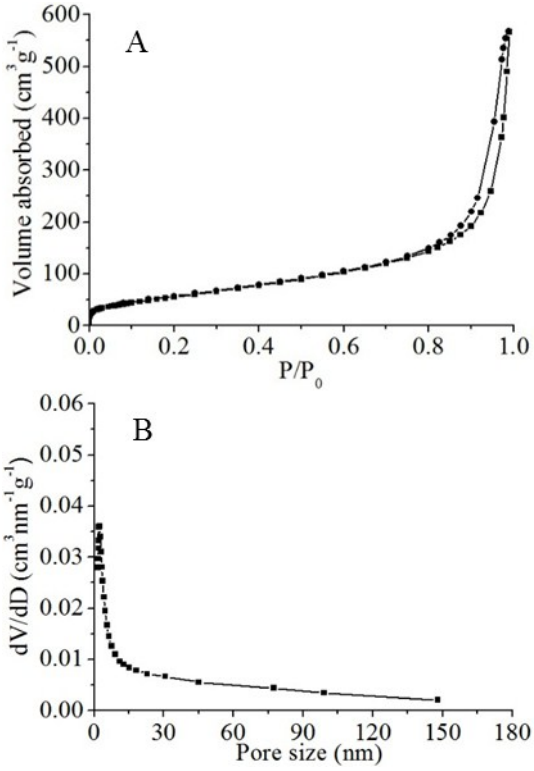

Figure S7. N_2 adsorption and desorption (A) and BJH adsorption pore size distribution (B) of Ni/Ni-Al_2O_3.

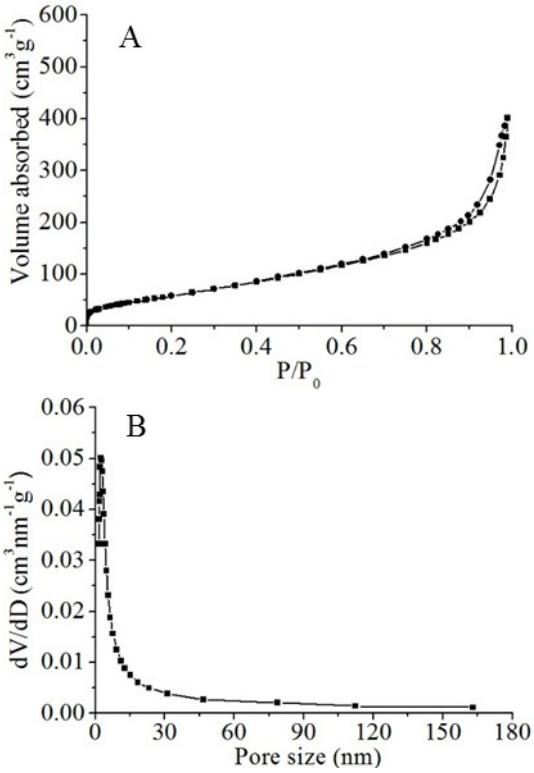

Figure S8. N_2 adsorption and desorption (A) and BJH adsorption pore size distribution (B) of Ni/Al_2O_3.

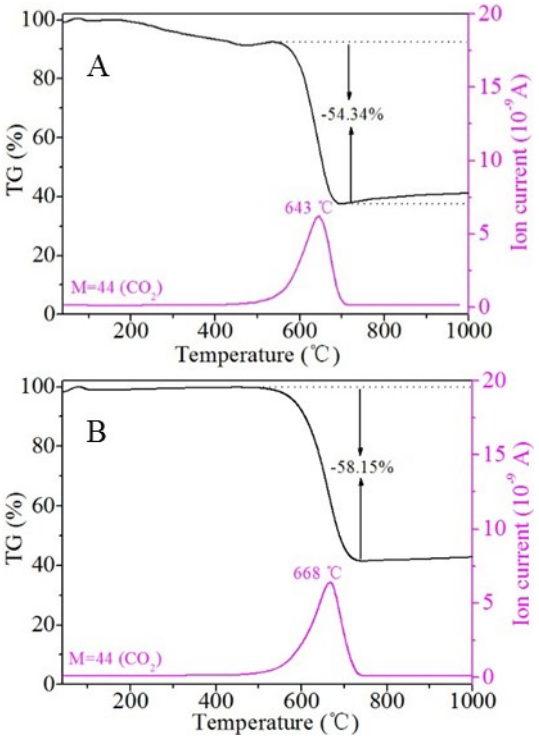

Figure S9. TG-MS profiles of the used catalysts of Ni/Al_2O_3 (A) and $Ni/Ni\text{-}Al_2O_3$ (B) after reacted for 14 and 80 h, respectively.

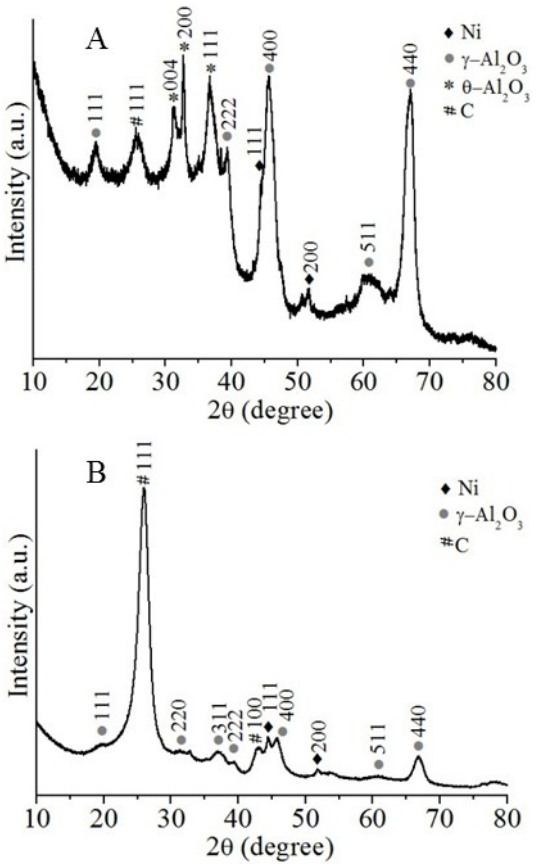

Figure S10. XRD patterns of the used catalysts of Ni/Al_2O_3 (A) and $Ni/Ni\text{-}Al_2O_3$ (B) after reacted for 14 and 80 h, respectively.

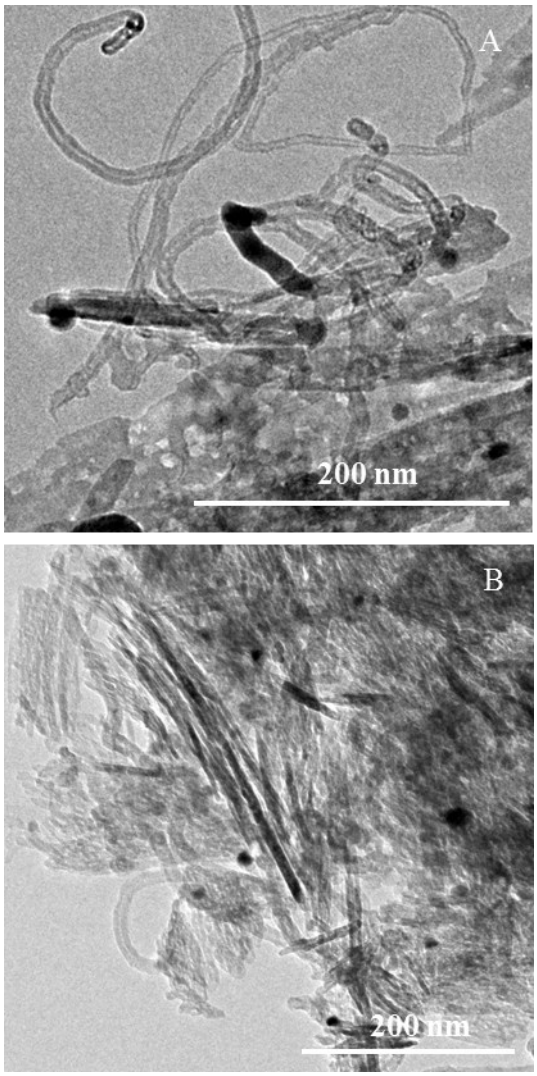

Figure S11. TEM image of the used catalysts of Ni/Al_2O_3 (A) and $Ni/Ni\text{-}Al_2O_3$ (B) after reacted for 14 and 80 h, respectively.

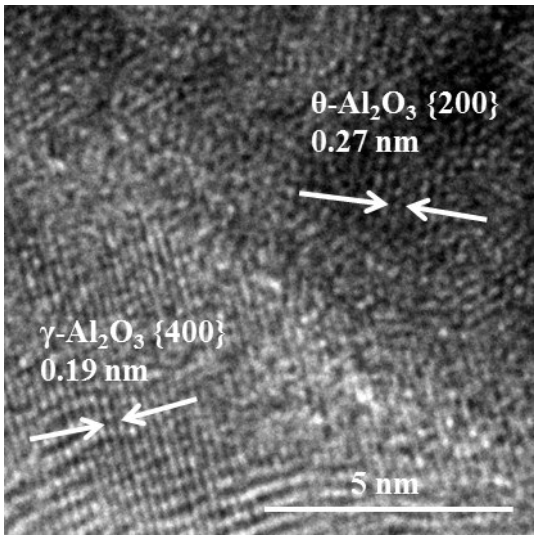

Figure S12. HRTEM image of the used Ni/Al_2O_3 catalyst after reacted for 14 h.

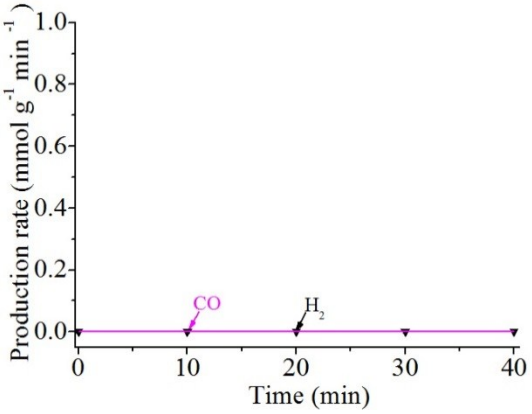

Figure S13. Time course of CO and H_2 production rates for photocatalytic CRM on $Ni/Ni\text{-}Al_2O_3$ at near room temperature under the UV-Vis-IR irradiation.

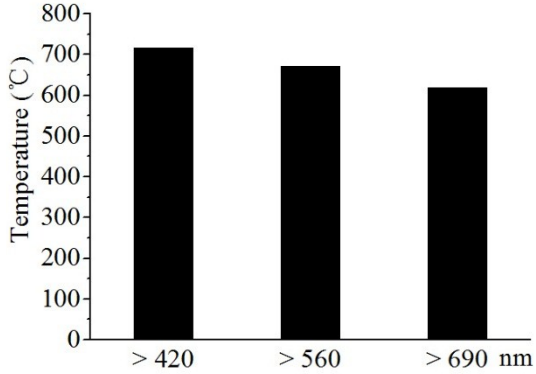

Figure S14. The equilibrium temperatures of Ni/Ni-Al_2O_3 under the focused Vis-IR irradiation.

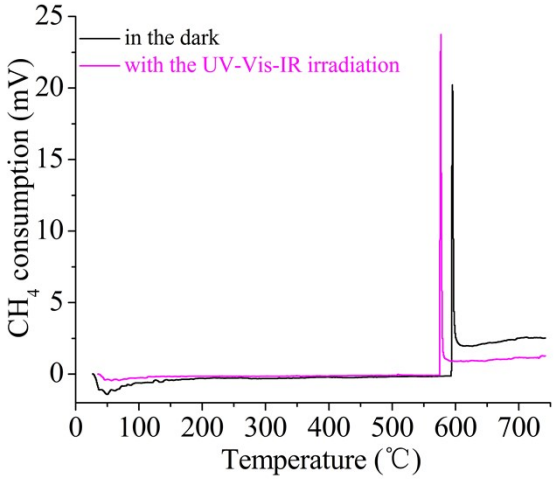

Figure S15. The CH_4-TPD profiles of Ni/Ni-Al_2O_3 under the UV-Vis-IR irradiation and in the dark.

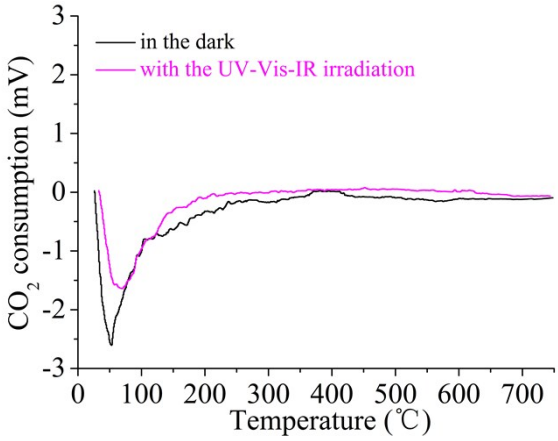

Figure S16. The CO_2-TPD profiles of Ni/Ni-Al_2O_3 under the UV-Vis-IR irradiation and in the dark.